Parametric Study, Simulation and Optimization of a Friction Stir Welding

T.Pavan Kumar[1] Ramanjaneya Reddy Munnangi[2] Madhu Anupoju[3] Lavu Gopi Nath[4]
[1]Assosiate Professor [2,3]Student [4]Assistant Professor
[1,2,3,4]Department of Mechanical Engineering
[1,2,3]Nalla Narasimha Reddy Education Society's Group of Institutions [4]St. Peter's Engineering College

Abstract— This thesis research implemented an existing thermo mechanical model of friction stir welding process, and studied the surrogate model-based optimization approach to obtain optimal process parameters for the modelled friction stir welding process. As an initial step, the thermo mechanical model developed by Zhu and Chao for friction stir welding of 304L stainless steel was replicated using ANSYS. The developed model was then used to conduct parametric studies to understand the effect of various input parameters like total rate of heat input, welding speed and clamping location on temperature distribution and residual stress in the work piece. With the data from the simulated model, linear and nonlinear surrogate models were constructed using regression analysis to relate the selected input process parameters with response variables. Constrained optimization models were formulated using surrogate models and optimization of process parameters for minimizing cost and maximizing throughput was carried out using improved harmony search algorithm. To handle the constraints, Deb's parameter-less penalty method was used and implemented in the algorithm. It is learned from this research that: (1) heat input is mainly constrained by the lower bound of the temperature for making good welds; (2) the optimal welding speed must balance the loss of heat input and the gain in productivity; (3) clamping closer to the weld is better than away from the weld in terms of lowering the peak residual stresses. Moreover, the nonlinear surrogate models resulted in a slightly better optimal solution than the linear models when wide temperature range was used. However, for tight temperature constraints, optimization on linear surrogate models produced better results. The implemented improved harmony search algorithm seems not able to converge to the best solution in every run. Nevertheless, the non-converged solution it found was very close to the best.

Key words: FSW, Friction Stir Welding

I. INTRODUCTION

Friction Stir Welding (FSW) is a revolutionary solid state welding technique invented at The Welding Institute (TWI) in 1991 [1]. The FSW process operates below the solidus temperature of the metals being joined and hence no melting takes place during the process. This process is a derivative of the conventional friction welding and is being used to produce continuous welded seams for plate fabrication [2]. Since its invention in 1991, continuous attempts have been made by researchers to understand, use and improve this process. Friction Stir Welding is a hot-shear joining process in which a non-consumable, rotating tool plunges into a rigidly clamped work piece and moves along the joint to be welded [3]. The cylindrical rotating tool used in FSW has a profiled threaded or unthreaded probe of length less than the weld depth, extruding from the tool shoulder. The operating principle of FSW process is presented in figure 1.1.
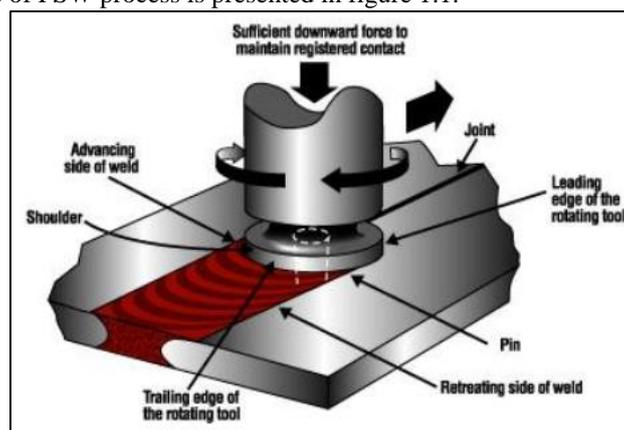

Fig. 1.1: Friction Stir Welding Operation Principle

II. THERMO MECHANICAL MODEL OF FSW

The Finite Element Method (FEM) offers a way to solve complex continuum problems by subdividing it into a series of simple interrelated problems. FEM is most commonly used in numerical analysis for obtaining approximate solutions to wide variety of engineering problems [48]. In the present study, a commercial general purpose finite element program ANSYS® 11.0 was used for numerical simulation of friction stir welding process.

The purpose of the thermal model is to calculate the transient temperature fields developed in the work piece during friction stir welding. In the thermal analysis, the transient temperature field T which is a function of time t and the spatial coordinates (x, y, z), is estimated by the three dimensional nonlinear heat transfer equation (2.1).

$$k \left(\frac{\partial^2 T}{\partial x^2} + \frac{\partial^2 T}{\partial y^2} + \frac{\partial^2 T}{\partial z^2} \right) + Q_{int} = c\rho \frac{\partial T}{\partial t} \qquad (2.1)$$

Where k is the coefficient of thermal conductivity, Q_{int} is the internal heat source rate, c is the mass-specific heat capacity, and ρ is the density of the materials [28, 50]. The heat transfer model developed for the thermal analysis is described in the following section.
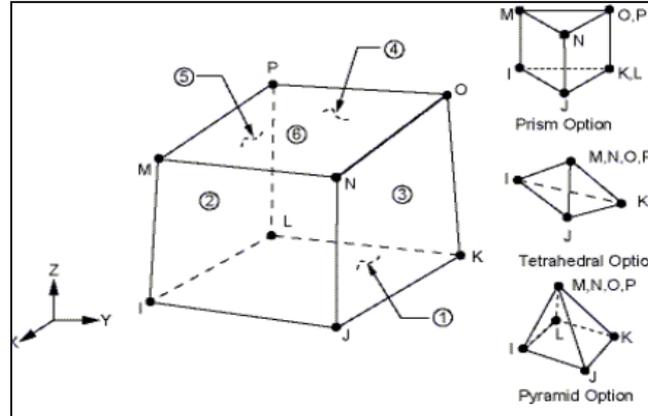

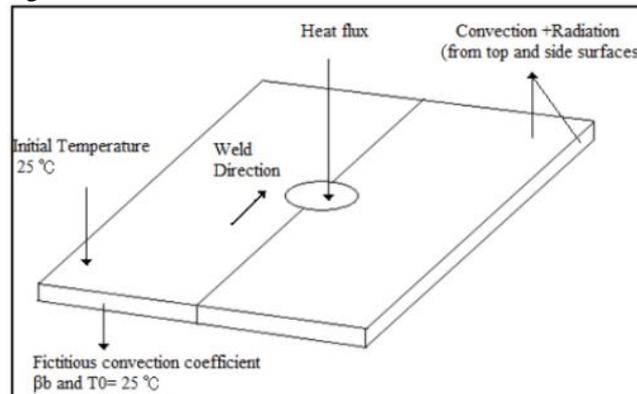Fig. 2.1: Three dimensional surface effect element SURF152

Fig. 2.2: Schematic representation of boundary condition for thermal analysis

A. Boundary Conditions

In the present analysis, sequentially coupled finite element analysis is carried out. The temperature histories obtained from thermal analysis are applied as body loads in the mechanical analysis. The forces from the thermal expansion of the work piece material are the only forces considered in this analysis.

The following boundary conditions are utilized for the mechanical analysis:
- The work piece is constrained of vertical motion at the bottom surface.
- The work piece is fixed through clamping by 304.8 mm long L-shaped steel strip (25.4 mm x 25.4 mm x 6.35 mm) on each plate at a distance 50.8 mm from the weld centre. Totally rigid boundary conditions are applied at these clamping locations. The clamping constraints are released after the weld cools down to room temperature.
- There are no displacements along the symmetric surface.

B. Validation of Thermo mechanical Model of Friction Stir Welding

For validating the thermo mechanical model developed using ANSYS®, it was essential to correlate the developed model with the published results. For this purpose, the developed thermo mechanical model was verified with numerical results obtained by Zhu and Chao [28].

C. Temperature Responses

Measurement of temperature was made by Zhu and Chao [28] through the use of 36 gauge k Type thermocouples embedded at nine locations on the top and bottom surface along the transverse section of the work piece. The graph in figure 5.1 shows the comparison of instantaneous experimental and simulation results for top surface of work piece.
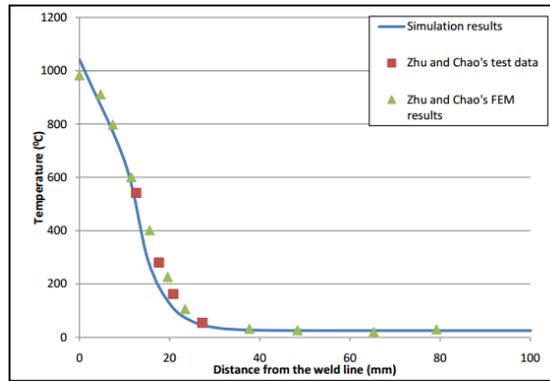
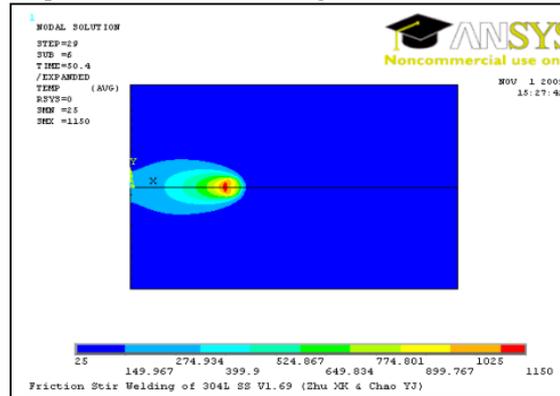Fig. 2.3: Comparison of temperature distribution along the transverse direction at welding time t= 83 s

Fig. 2.4: Temperature distribution on top surface of the work piece at welding time, t= 50.4 sec

D. Stress Responses

The temperature fields obtained from the thermal model are used as input for the mechanical simulation for calculation of residual stresses. The primary residual stresses in FSW were observed in the longitudinal direction. Therefore, only longitudinal stresses were considered in this study. Figure 5.4 shows the comparison of results from Zhu and Chaos model [28] and simulation results of longitudinal residual stresses for the top surface. The residual stresses were measured along traverse direction at a distance of 152 mm from the end of the work piece. Fixture release was modelled in order to estimate the effect of clamping. It was observed that the residual stress in the welds decreased significantly after the fixture release. The overall trend of the developed model for prediction of residual stress is similar to that of Zhu and Chao [28], thus verifying the validity of the model developed in this study.
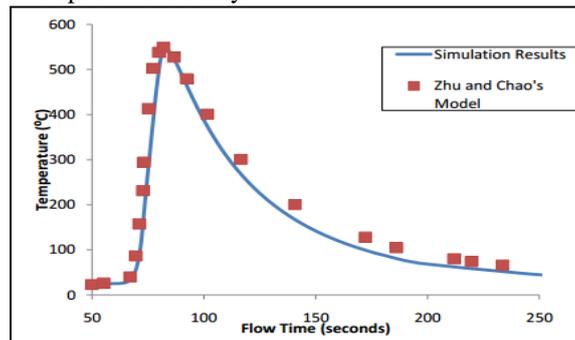

Fig. 2.5: Variation of transient temperature - comparison of simulated results and results from Zhu and Chaos Model Figure
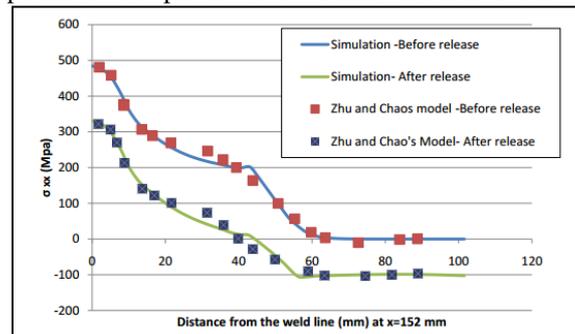

Fig. 2.6: Variation of the longitudinal residual stress along the traverse direction at the middle section of the work piece

III. PARAMETRIC STUDY AND SURROGATE MODELS OF FSW PROCESS

In order to conduct parametric investigation of FSW process, design of experiment methodology is implemented in this study. Design of experiment (DoE) technique is used to optimize the number of experiments required to determine the effects of various factors affecting the response of the system [56]. DoE helps to eliminate the need for extensive experimental analysis and in turn reduces the computational time and cost. The following sections describe the details of DoE and development of surrogate models for FSW process.

Response	Process Parameters	Units	Range	Level 1	Level 2	Level 3	Level 4	Level 5
Temperature (T)	Weld Speed (S)	mm/sec	0.5-2.54	0.5	0.85	1.00	1.69	2.54
	Heat Input (H)	watt	500-970	500	600	760	970	-
Residual Stress (R)	Weld Speed (S)	mm/sec	0.5-2.54	0.5	0.85	1.00	1.69	2.54
	Heat Input (H)	watt	500-970	500	600	760	970	-
	Clamping location (C)	mm	50.2-76.2	50.2	76.2	-	-	-

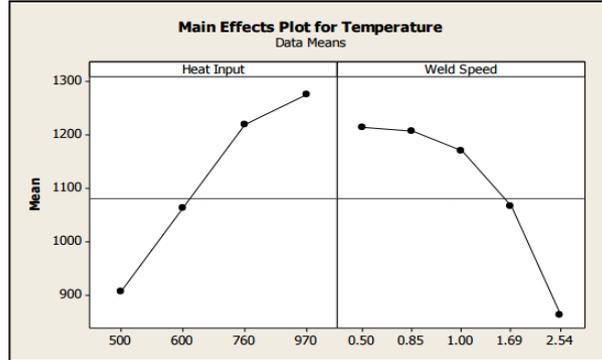Table 4.1: Process parameters, range and design levels used

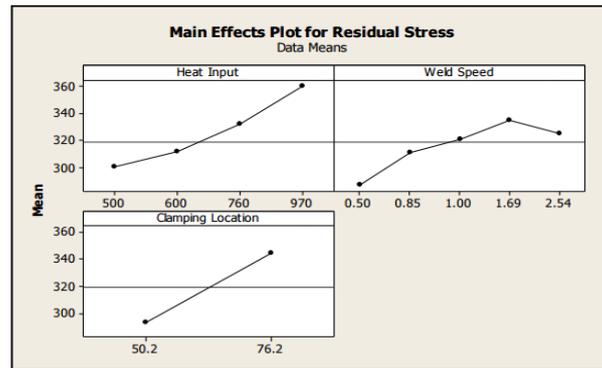Fig. 4.1: Plot of main effects for temperature

Fig. 4.2: Plot of Main Effects for Residual Stress

Figures 4.1 and 4.2 depict the plots of main effects for temperature and residual stress, respectively. These plots help to assess the effect of each factor graphically. The figures 4.1 and 4.2 show that heat input factor has a significant effect on both temperature and residual stress and a direct proportionality can be seen between the heat input factor and the responses. Temperature decreases with increasing welding speed. Figure 4.3 shows the variation of temperature on top surface of the work piece for welding speeds 0.50 mm/s to 2.54 mm/s at constant heat input of 600 W. The peak temperature tends to increase as the welding speed is reduced. On the other hand, it is observed residual stress first increases with increase in welding speed and then tends to slightly decrease at higher welding speed
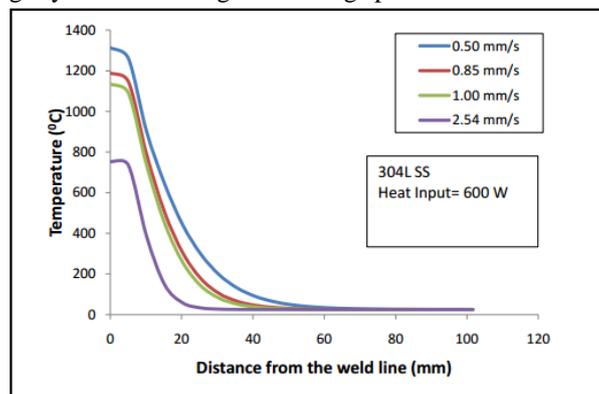

Fig. 4.3: Variation of temperature on top surface of the work piece at different welding speeds

IV. RESULTS AND DISCUSSIONS

In order to validate the optimization results, finite element analysis (FEA) simulations were carried out according to the process parameters that were obtained from the optimization scheme. Table 5.1 presents the summary of optimal results obtained for different cases for response variable, temperature. The results indicate that the developed models were able to predict the temperature with a reasonable accuracy.

		Temperature Constraint Range		
		1000-1300	1050-1150	1140-1150
Optimal Solution	Heat Input (W)	808.50	855.678	931.576
	Weld Speed (mm/s)	2.54	2.54	2.54
Model	Best Model	Model 2	Model 2	Model 1
	Regression Type	Nonlinear	Nonlinear	Linear
Output Temperature ℃	Model Predicted	999.9998	1050.001	1140.0
	FEA Simulation	977.678	1029.43	1112.8
	Error %	2.2831	1.9982	2.4442

Table 5.1: Summary of results for Response – Temperature

The figure 5.1 shows the temperature contour at the selected location i.e. X=152.4, Y=0, and Z=0 for the optimal parameters corresponding to temperature constraint range 1000-1300℃. The peak temperature obtained with optimal parameters as H= 808.5 W and S= 2.54 mm/s is 977.67℃, while that predicted by the best model is 999.99℃. The Model 2 in this case overestimated the temperature by about 2.28%. From table 5.1, it is seen that the corresponding temperature values of all the optimal solutions take on the lower bounds of temperature constraint.
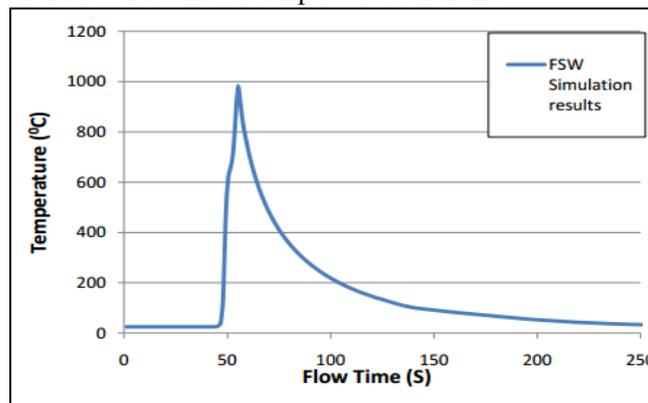

Fig. 5.1: Temperature profile at X=152.4, Y=0, Z=0 for optimal parameters H= 808.5 W and S= 2.54 mm/s

Model 3 and Model 4 have additional constraints on the maximum level of residual stresses that can be reached. Table 5.2 presents the summary of optimal results obtained for different cases for the two response variables, temperature and residual stress

			Temperature Constraint Range	
			1000-1300	1050-1150
Optimal Solution		Heat Input(W)	772.970	779.8538
		Weld Speed(mm/s)	2.312	2.162
		Clamping Location (mm)	50.2	50.2
Model		Best Model	Model 4	Model 4
		Regression Type	Nonlinear	Nonlinear
Output	Temperature ℃	Model Predicted	1021.618	1069.978
		FEA Simulation	991.216	1036.87
		Error %	3.0671	3.1930
	Residual Stress MPa	Model Predicted	309.9971	309.9973
		FEA Simulation	316.597	323.247
		Error %	-2.0846	-4.0989

Table 5.2: Summary of results for responses - temperature and residual stress

In order to validate the results for the optimization Model 4, thermo mechanical simulations were carried out. The figure 5.2 shows the temperature profile at the selected location i.e. X=152.4, Y=0, and Z=0 for the optimal parameters corresponding to temperature constraint range 1000 - 1300℃. The peak temperature obtained with optimal parameters as H= 772.97 W, S= 2.312 mm/s and C=50.2 mm is about 991.216℃, while that predicted by the best model is 1021.618 ℃.
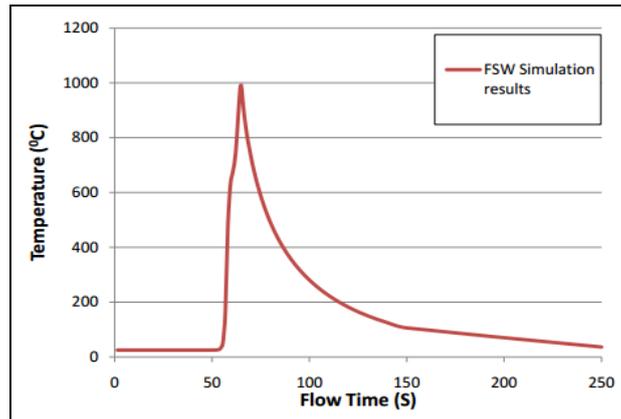
Fig. 5.2: Temperature profile at X=152.4, Y=0 m Z=0 for optimal parameters H= 772.97 W and S= 2.312 mm/s

The corresponding longitudinal residual stress developed during the process operating at the optimal parameters H= 772.97 W, S= 2.312 mm/s and C= 50.2 mm are shown in figure 5.3. The residual stresses on top surface are plotted at distance a distance of x =152.4 mm along the traverse direction. The residual stress obtained from FEA at the selected location X=152.4, Y=0, and Z=0 is about 316.597 MPa, while that predicted by the Model 4 is 309.997 MPa. It was observed that the clamping constraints had some localized effect on the stress components in the 0 200 400 600 800 1000 1200 0 50 100 150 200 250 Temperature (0C) Flow Time (S) FSW Simulation results 59 unaffected parent material [30]. Both the temperature and residual stress constraints are satisfied by the Model 4. The error in predicting the temperature is about 3.06%, while the error in predicting residual stress is about - 2.08%
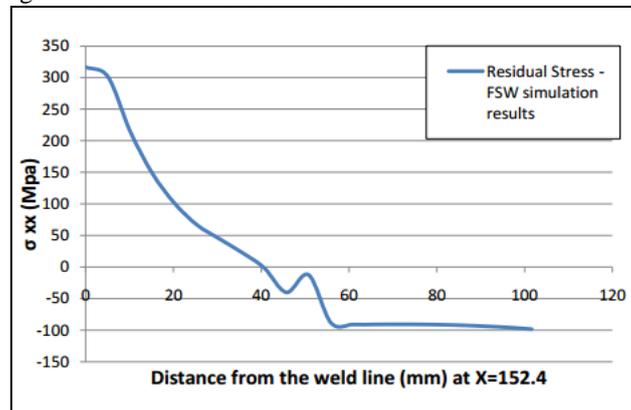

Fig. 5.3: Variation of the longitudinal residual stress along traverse direction operating at optimal parameters H= 772.97 W, S= 2.312 mm/s and C= 50.2 mm

V. CONCLUSIONS AND RECOMMENDATIONS FOR FUTURE WORK

In this research a thermo mechanical model of friction stir welding process was reproduced and a surrogate model-based optimization scheme was implemented to obtain the optimal parameters for the process. The thermo mechanical model selected for implementation was developed by Zhu and Chao for friction stir welding of 304L stainless steel. The selected finite element model was replicated using ANSYS® and validated with the published results. The validated model was then used to simulate the process. A design of experiments and parametric study were performed to identify the effect of various input parameters like: heat input, welding speed and clamping location on temperature distribution and residual stress in the work piece. Later, linear and nonlinear surrogate models were developed using regression analysis to relate the selected process input parameters with the response variables. Finally, constrained optimization models were formulated using surrogate models with the goal of maximizing throughput and minimizing cost under constraints of achieving desired weld quality and satisfying the operating constraints. The optimization problems were solved using the improved harmony search algorithm, enhanced with the parameter-less penalty method proposed by Deb to handle the constraints.

For future work, experimental investigations need to be carried out to verify the numerical simulations and optimal solutions obtained in this thesis. The process variables used in this study were limited to responses, maximum temperature and residual stress and the following input variables: heat input, weld speed, and clamping location. The optimization can be performed on a process model that includes more input process variables and output responses. The materials to be welded are considered identical in this study. Similar studies can be extended to other variants of friction stir welding processes such as laser-assisted friction stir welding process, or the welding of dissimilar materials that will be technically more challenging due to the differences in material properties. More comprehensive thermal-material-mechanical models could also be considered for optimization.

REFERENCES

[1] Thomas, W.M., Nicholas, E.D., Needham, J.C., Murch, M.G., Temple-Smith, P., and Dawes, C.J., Friction-stir butt welding, GB Patent No. 9125978.8, International patent application No. PCT/GB92/02203, (1991).

[2] Thomas, W.M., Threadgill P.L., and Nicholas, E.D., Friction stir welding of steel: Part one, http://steel.keytometals.com/default.aspx?ID=CheckArticle&NM=219.

[3] Nandan, R., DebRoy, T., and Bhadeshia, H., Recent advances in friction-stir welding - Process, weldment structure and properties. Progress in Materials Science, 2008. 53(6): p. 980-1023.

[4] Friction Stir Link Inc, http://www.frictionstirlink.com/fslfswdescription.html.

[5] Lienert, T.J., Stellwag, W.L., Grimmett, B.B., and Warke, R.W., Friction stir welding studies on mild steel - Process results, microstructures, and mechanical properties are reported. Welding Journal, 2003. 82(1): p. 1S-9S.

[6] Zettler, R., Donath, T., dos Santos, J.F., Beckman, F., and Lohwasser, D., Validation of marker material flow in 4mm thick frictionstir welded Al2024-T351 through computer microtomography and dedicated metallographic techniques. Advanced Engineering Materials, 2006. 8(6): p. 487-490.

[7] Sorensen, C.D. and Nelson T.W., Friction Stir Welding of Ferrous and Nickel Alloys, in Friction stir welding and processing, Mahoney, M. W. and Mishra, R.S., Editors. 2007, ASM International: Materials Park, Ohio. p. 111-121.

[8] Park, S.H.C., Sato, Y.S., Kokawa, H., Okamoto, K., Hirano, S., and Inagaki, M., Microstructural characterization of stir zone containing residual ferrite in friction stir welded 304 austenitic stainless steel. Science and Technology of Welding and Joining, 2005. 10(5): p. 550-556.

[9] Park, S.H.C., Sato, Y.S., Kokawa, H., Okamoto, K., Hirano, S., and Inagaki, M., Rapid formation of the sigma phase in 304 stainless steel during friction stir welding. Scripta Materialia, 2003. 49(12): p. 1175-1180.

[10] Ozekcin, A., Jin, H.W., Koo, J.Y., Bangaru, N.V., Ayer, R., Vaughn, G., Steel, R., and Packer, S., A microstructural study of friction stir welded joints of carbon steels. International Journal of Offshore and Polar Engineering, 2004. 14(4): p.284-288.